e-Prime - Advances in Electrical Engineering, Electronics and Energy 4 (2023) 100151

Contents lists available at ScienceDirect

e-Prime - Advances in Electrical Engineering, Electronics and Energy

journal homepage: www.elsevier.com/locate/prime

Flexible horizontal piezoelectric energy generator for sea wave applications

A.S. Deraman [a], M.R. Mohamed [a,*], W.I. Ibrahim [a], P.K. Leung [b]

[a] Faculty of Electrical and Electronics Engineering Technology, Universiti Malaysia Pahang, Pekan 26600, Malaysia
[b] Renewable Energy, Chongqing University, 400044, China

ARTICLE INFO

Keywords:
Energy harvesting
Flexible horizontal piezoelectric
Bimorph piezoelectric
Sea wave
ANSYS

ABSTRACT

Energy harvesting from the environment becomes a valuable technology, especially for sea wave applications, in which it usually ends up wasted despite its potential to be harvested. Due to its wide availability and high energy density, piezoelectric energy harvesting (PEH) is becoming popular for flexible energy harvesting. This paper presents a flexible horizontal piezoelectric (FHP) energy harvester to harvest energy from the surface of sea wave. The harvester is made of bimorph piezoelectric devices; they are utilised to amplify and convert the collected mechanical vibrations into electrical power. A finite element model is established from ANSYS simulations to solve the iteration method by generating resonance frequency (f_r). Then, Taguchi method, SN ratio and the ANOVA approach were used by considering the input variable of f_r to estimate the optimum performance through control factors; number of blade, length and thickness. From the performance test result, it is proven that the higher numbers of blade including length, and minimum numbers of thickness significantly improve the significant level, $\alpha = 0.05\%$ of ANOVA. Three prototypes are developed with approximate body dimensions through the resonance frequency perform and generate a 160.3 Hz on blade dimensions of $10 \times 300 \times 0.2$ mm, with a piezoelectric (PZT) on its surface. This particular study shows that the potential of output power is generated from sea wave surface through a significant relationship between length, thickness, and blade design. This research develops a novelty for energy harvesting from flexible piezoelectric generator on sea wave application that could be easily install on offshore platform.

1. Introduction

Nowadays, conventional energy sources such as oil, coal, and natural gas, also known as fossil fuels, contribute to the greenhouse effect. Global energy demand will grow continuously by 56 % forecast from 2010 level by 2040 [1]. To minimise the global warming crisis and reduce carbon emissions, it is necessary to decrease the uses of fossil fuels while increasing the use of renewable energy sources. The utilisation of such energy harvesting for delivering power becomes particularly crucial for systems where batteries are difficult to swap or replenish [2,3].

Ocean wave energy is one of the most abundant energy sources in this world. Afsharfard et al. [4], state that ocean wave energy is a stable renewable energy source and has great application possibilities. This energy has the potential to replace the current use of non-renewable energy sources as it is considered as the cleanest, renewable, and most predictable than solar and wind powers. The advantages of using ocean energy sources over other renewable energy sources [5] are abundance, availability, high load factor, lower environmental impact and source predictability. Furthermore, ocean energy has additional benefits in term of longer service life on wave energy generation equipment and very efficient renewable and natural energy sources to be consumed.

Various forms of vibration energy source from ocean waves have been studied to harvest the electrical energy, such as tidal energy [6], mechanical vibrations [7], pelamis [8], etc. As one of the aforementioned energy sources, mechanical vibration energy through ocean waves has recently gained significant attentions, it is prevalent in environment where solar or heat energy cannot be used. These mechanical vibrations can be converted into electrical energy through a variety of conversion techniques, including piezoelectric effect [9], triboelectric effect [3], dielectric effect [10], electrostatic effect [11], etc. The piezoelectric effect has drawn a lot of its advantages among the conversion mechanisms, including high power density, low cost, and easy of miniaturization.

Meanwhile, piezoelectric transduction is one of the commonest mechanical energy harvesting techniques. Because of its high electromechanical coupling factor and piezoelectric coefficient when compared to electrostatic, electromagnetic, and triboelectric transductions, the scientific community is very interested in piezoelectric energy

* Corresponding author.
E-mail address: rusllim@ump.edu.my (M.R. Mohamed).

https://doi.org/10.1016/j.prime.2023.100151
Received 2 January 2023; Received in revised form 5 March 2023; Accepted 5 April 2023
Available online 6 April 2023

Acronyms

f_r	Resonance Frequency
α	significant level
d	Depth
λ	Wavelength
g	Ocean gravity
a	Wave amplitude
t	Time
n	Wave number
ω	Angular frequency
f	Stiffness elastic
e	Piezoelectric matrix
ε^T	Permittivity dielectric
T	Matrix transpose
S	Strain vector
N	Vector stress
M	Flux density
D	Field intensity
e^T	Electric strain constant
η	Surface displacement
Z	Ocean wave amplitude
L	Wave length
w	Wave number
T	Wave period
θ	Angular displacement
ε	Strain
δ	Distance of PZT
ρ	Curvature radius of PZT
V_o	Output voltage
A_i	Area of piezoelectric blade
n_p	Number of piezoelectric blade
P	Output power
R_o	External resistance
V_i	Voltage every blade
d_{31}	Piezoelectric effect
PVDF	Polyvinylidene Fluoride
PZT	Lead Zirconate Titanate
PUR	Polyurethanes

harvesting [12]. Therefore, the natural resonant frequency is a typical energy harvesting structure in the piezoelectric cantilever [13]. Moreover, the energy density for piezoelectrics is three times higher [14] than those for electromagnetic transduction and electrostatics, which are studied extensively. Even with the inconsistency of ocean waves, the output power is still predictable and smoother than wind and solar.

Because of the benefits of piezoelectricity, research into piezoelectric mechanics and energy harvesting has grown in recent decades. When a piezoelectric material is being pressure, the atomic structures of the material change. It causes the variance formation of the material's dipole moment and voltage to be different, and this phenomenon is called direct piezoelectric effect [15]. Meanwhile, two main groups of piezoceramics underlie piezoelectric materials with a high electromechanical coupling coefficient and piezopolymers with appropriate flexibility. Polyvinylidene Fluoride (PVDF) and Lead Zirconate Titanate (PZT) are classified into the common piezoelectric polymers and ceramics, respectively [16]. Furthermore, harvest energy using piezoelectric materials is possible since there are many periodic external forces elsewhere. In addition, piezoelectric materials are among the promising choices for harvesting energy from ocean waves and wind by utilizing a variety of methods and technologies.

The idea of using the piezoelectric effect of ocean waves for energy harvesting was proposed in the 1970s and has been further explored so far [17]. The generated electrical power from the wave of piezoelectric effect energy harvesting shows that the mean value during power production increased by having the ratio of the width to thickness of the cantilever, sea depth, wave height, ratio mass to cantilever mass, and ratio of sea depth to the wave length [18,19]. Cui et al. [20] studied the flexible sandwich structure of piezoelectric seaweed, calculating the output power by using ANSYS. Nevertheless, the limitations of blade design and low deformation of water flow caused relatively weak output voltages. Zhao et al. [21] used ANSYS to create output power for a design method by including cantilever beam construction with low frequency. Therefore, PZT piezoelectric material was often chosen due to its high-volume dielectric constant and coefficient. Xie et al. [22] used PZT piezoelectric transducers to investigate the potential of energy harvesting with longitudinal and transverse motion from ocean and sea waves.

Models of elastic beams with Airy linear wave theory were extracted using mathematical equations. Wu et al. [14] proposed two horizontal cantilever beams for floating structures that were connected to a PZT piezoelectric patch for the ocean wave transverse motion. Furthermore, Viet et al. [23] designed a floating mass-spring device with two piezoelectric levers with anchor rope to harvest energy from intermediate and deep water waves. Nevertheless, the harvesting systems are mostly complex, such as their size and the challenge of allocating them at different locations. Mutsuda et al. [24] experimental studied to harvest energy from ocean wave by using piezoelectric paint with flexible device coating. Unfortunately, it is covered in intermediate water and should be examined in real sea conditions in deep water to test the durability and reliability.

Two simultaneous of particle motion inside of wave; longitudinal and transverse motion are caused by the particles of water near the free surface. The particles move in circular and elliptical path, which contribute to intermediate and deep water waveforms; this is called Airy linear wave theory [19]. Besides, it is part of the determining factor in applying the force and activating the energy harvesting mechanisms in the water waves. In addition, the steady operation and easy evaluation for maintenance and replacement of a harvesting system in an ocean environment are the hurdles for absorbing efficient energy, particularly using piezoelectric technology.

At present, numerous models have been developed to investigate energy harvesting through transverse waves of piezoelectric effects. Nevertheless, little work has been carried out to harvest maximum energy from appropriate orientations of piezoelectric cantilever beam and previous works have not comprehensively considered on multiple flexible horizontal beam model. Therefore, substantial study on the flexible horizontal piezoelectric of the individual component with multiple generators for absorbing electrical energy is necessary. Furthermore, the application of the first layer of transverse motion is essential in order to develop a model to understand the relative importance of the flexible device in energy harvesting. The remainder of this article is organized as follows: Section 2 presents the methodology adopted to carry out the study. The results obtained and their discussions are presented in Section 3. The conclusion ends the paper in Section 4.

2. Materials and methods

2.1. Flexible cantilever design

Fig. 1(a) illustrates a FHP on top of a sea wave, consisting of multi-directional transverse wave motion. The FHP is composed of a flexible cantilever structure and is attached to the base unit of the piezoelectric module. The PZT material was selected due to its high volume dielectric

(a)

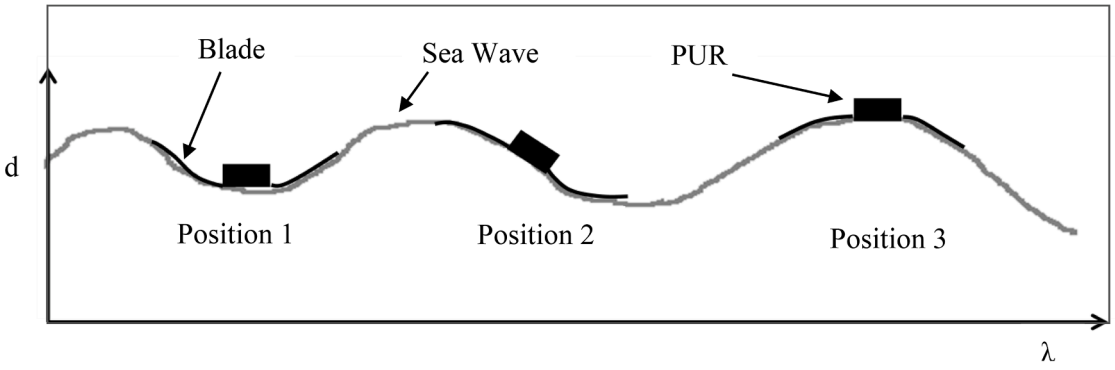

(b)

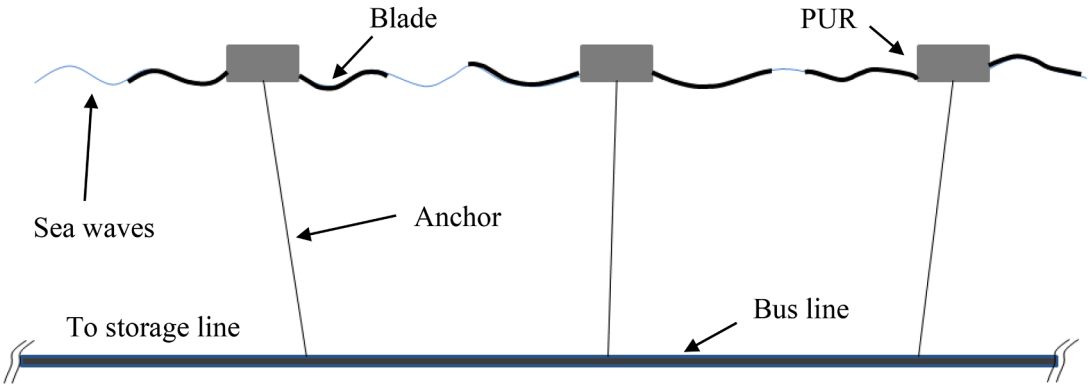

(c)

Fig. 1. Illustration of FHP energy harvester (a) propose FHP model on sea wave (b) schematic of the movement of the FHP with different phase motion of sea wave phase operation and (c) FHP with storage and anchoring type.

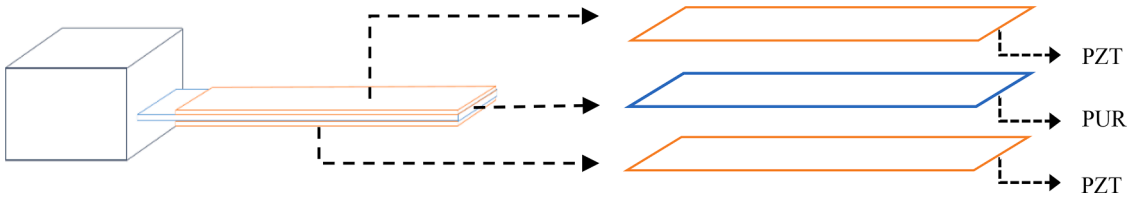

Fig. 2. Typical laminated blade structure for bimorph of FHP.

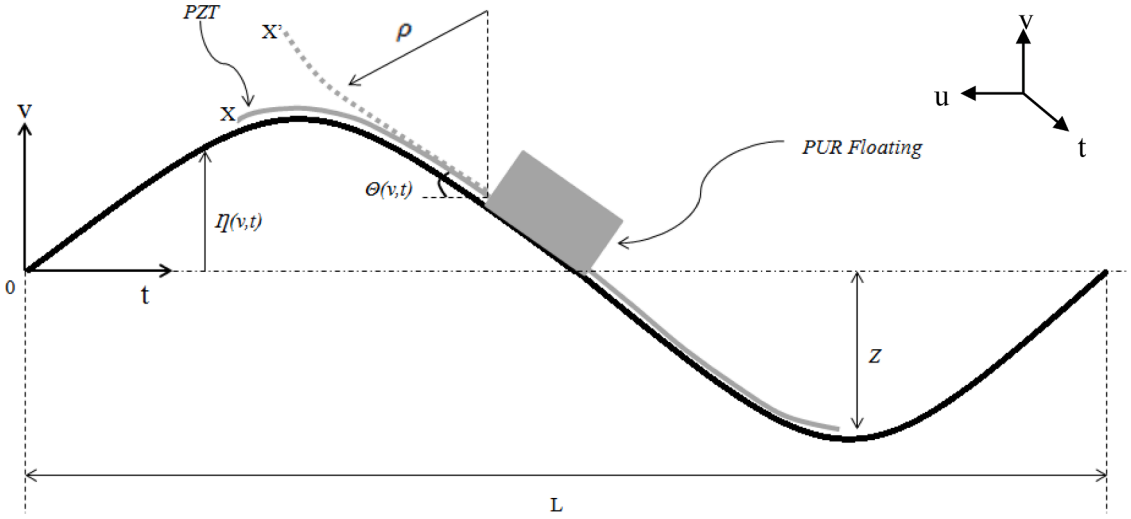

Fig. 3. A profile sketch of the FHP on transverse wave motion.

constant and coefficient [21] and placed on top of the blade to absorb the deformation by external force of transverse wave motion. Piezoelectric blades are attached to polyurethanes (PUR) as a floating body on transverse motion from wave particles. Multiple blades are proposed since the wave directions are different to convert the oscillatory nature of the sea waves from kinetic energy into electricity.

According to Fig. 1(b), three possible phase operations of FHP depending on the transverse wave operation. The depth (d) versus wavelength (λ) of a sea wave brings the fluid particles moving constantly up and down by varying the displacement and acceleration. The relative displacement required to trigger oscillations of different positions during acceleration. The proposed model is designed to float on the sea surface. Furthermore, the harvester's operations required anchoring for safety and control of movement of FHP to float freely. However, the operation allows free moving; and self-mobilization extracts energy when conditions are within a predetermined safety zone. Fig. 1(c) depicts the proposed model with anchoring and output generated from FHP connected to the bus line for storage under off-grid connections. In addition, the storage could store energy in a battery to have self-powering storage.

The blade design is composed of a minimum of two blades and a maximum of six blades for each model. Typically, each blade is laminated with a bimorph of piezoelectric material of varying thickness and length based on the dimensions properties. The piezoelectric material was coated on top and bottom sides of the blade with flexible material (PUR). Fig. 2 shows an illustration of the theoretical model for laminate structure in blade design.

The entire blade was coated in PZT materials to absorb as much energy as possible. Therefore, a suitable blade design must be selected to considering the mechanical force and rigidity of devices. In addition, the illustration was transformed into a numerical analysis to examine the characteristics of the deformation results.

2.2. System modeling and numerical simulations

A mathematical model was developed to describe the principle of operation of the flexible piezoelectric in transverse wave motion. Fig. 3 depicts the transverse wave motion of a piezoelectric energy harvester, consisting of flexible PZT and PUR on horizontal patches, subjected to wave particles. In this research, transverse wave motion is used to compare with its longitudinal one since directions of FHP displacements propagate in *v-t* plane. The fluid velocity; component for shallow water waver can be expressed as follows [25];

$$u = \frac{gak}{\omega}\left[\frac{\cosh(ky+kh)}{\cosh(kh)}\right][\cos(kx) - \cos(\omega t)] \tag{1}$$

$$w = \left[\frac{gak}{\omega}\right]\left[\frac{\sinh(ky+kh)}{\sinh(kh)}\right][\sin(kx) - \sin(\omega t)] \tag{2}$$

where a is the wave amplitude, t is time, n is wave number, and ω is angular frequency.

Furthermore, the finite element matrix equation for the piezoelectric effects is defined as follows:

$$N = (f)[S] + (e)[D] \tag{3}$$

$$M = (e)^T[S] + (\varepsilon^T)[D] \tag{4}$$

where f is the stiffness elastic, e is the piezoelectric matrix, ε^T is the permittivity dielectric (m/F) and T is the matrix transpose. S is the strain vector (N/m^2), N is the vector stress (m^2/N), e is the electric strain constant, M is the flux density, ε^T is the permittivity dielectric (m/F) at $T = 0$, T is the matrix of piezoelectric (Vm/N or m^2/C) and D is field intensity (V/m).

The surface displacement of sea wave particles, $u = \eta(v, t)$, is a function of the position, v, and time, t, which is depicted in Fig. 3.

The surface displacement of sea waves can be expressed as below

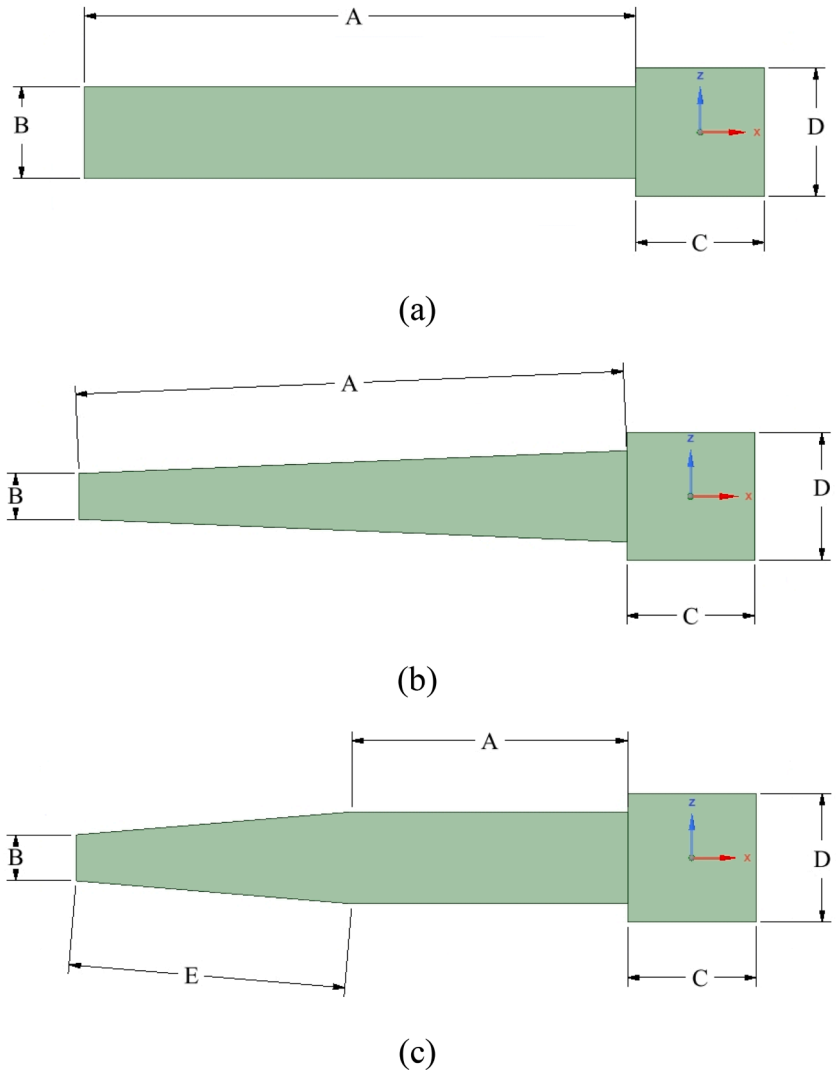

Fig. 4. Simulated models and their respective dimension (a) rectangular blade, (b) trapezoidal blade, and (c) stingray blade; with T varied from 0.2 mm – 1.0 mm, and L varied from 60 mm – 300 mm.

[23];

$$\eta(v,t) = Z{\cdot}\sin(w{\cdot}v - \omega{\cdot}t) \tag{5}$$

where Z is the wave amplitude. Substituting $w = 2\pi/l$ and $\omega = 2\pi/T$ into (5), the following equation can be obtained;

$$\eta(v,t) = Z{\cdot}\sin\left(\left(\frac{2\pi}{l}\right){\cdot}v - \left(\frac{2\pi}{T}\right){\cdot}t\right) \tag{6}$$

The angular displacement of FHP, $\theta(v, t)$, shown in Fig. 3 can be represented as;

$$tan\theta = \frac{d\eta(v,t)}{du} = Z{\cdot}w{\cdot}\cos(w{\cdot}v - \omega{\cdot}t) \tag{7}$$

$$\theta(v,t) = tan^{-1}(Z{\cdot}w{\cdot}\cos(w{\cdot}v - \omega{\cdot}t)) \tag{8}$$

Deformation of the FHP along the η are being measured through the curvature and distance of the piezoelectric. Therefore, differentiated values of strain along FHP could generate the elongation of the line segment. Furthermore, the strain, ε of PZT is as follows;

$$\varepsilon = \frac{\Delta dx'}{dx} = \frac{\delta}{\rho} \tag{9}$$

where δ is the distance of PZT, and ρ is the curvature radius of PZT element in which direction is along X-direction. The output voltage of V_o by using Eq. (9) as shown in Fig. 3 is as follows;

$$V_o = \frac{d}{dx}\int \varepsilon A_i$$

$$V_o = \frac{d}{dx}\int \frac{\delta}{\rho} A_i \tag{10}$$

where V_o is the output voltage, A_i is the area of i elements. From Eq. (10), the total output voltage, V_T is determined by;

$$V_T = \sum_{i=1}^{n} V_o \tag{11}$$

where V_T is the sum of the voltage V_o, where V_o is the voltage from every blade and n is the number of blade element. Hence, the deformation of PZT increases when the frequency and vibration is high, and the distance δ of PZT blade is needed to maximize electric power. The piezoelectric energy's output power is found by;

$$P = \frac{V_i^2}{2R_o} \tag{12}$$

where P is the output power, V_i is the voltage from every blade and R_o is

Table 1
FHP's dimension with A-E point varies of dimensions 60 – 300 mm of model.

	Dimensions (mm)				
Model	A	B	C	D	E
Rectangular	60 ~ 300	10	14	14	-
Trapezoidal	60 ~ 300	5	14	14	-
Stingray	30 ~ 150	5	14	14	30 ~ 150

Table 2
The parameters of FHP are used in numerical simulation research with density of PZT 7500 kg/m^3.

Properties	Float (PUR)	Flexible Piezo (PZT)	Units
Young's modulus	0.0075	1.7×10^{-5}	Gpa
Density	75	7500	kg/m^3
Poisson's ratio	0	0.3	
Permittivity Constant		8.85E-12	A^2·Sec^4/kg·m^3
PIEZ e31		-5.2	A·Sec/m^2
PIEZ e33		15.1	A·Sec/m^2
PIEZ e15		12.7	A·Sec/m^2
DPER ep11		729	
DPER ep33		635	

the constant value of external resistance. In additions, the piezoelectric effect mode of d_{31}, were used since the sea wave operation is directly proportional to the PZT material.

Three different models are proposed: rectangular, trapezoidal, and stingray-tail. Initially, 15 arrays were selected to obtain the optimum design for the energy harvested. Each model consists of different factors; 60 mm ~ 300 mm for length (L) and 0.2 mm ~ 1.0 mm for thickness (T). The variation factors are required to obtain the optimum value of S/N ratio that will be discussed in result and discussion.

Fig. 4 depicts all considered FHP models. It should be noted that the entire design model will be simulated in the numerical software that will be presented in the next section.

In previous research studies [26,27], two models were attempted; rectangular and trapezoidal, by using a numerical method to harvest the energy. The data was carried to observe the design through PZT material to achieve higher efficiency and performance. The proposed design has a 'tapered' at front (B) area to attain a constant strain level along the entire length of the cantilever beam. In addition, designs with different shapes of tapered also been explored. As mentioned, Fig. 4 (a)–(c), have different kinds of proposed designs in which, every blade is a bimorph cantilever that used serial connection of ceramic materials. The dimensions of the FHP in the simulations are given in Table 1.

Multiple dimensions are used to produce different displacement frequencies. The floating bases; C and D with a thickness of 2.5 mm, and the length of cantilever from end to end; A, B, and C, with a thickness are varying from 0.2 mm to 1.0 mm, respectively. According to wave energy conversion (WEC) theory, the floating units on the surface of wave water are moved to the motion of the incident wave and considered as wave profile devices with oscillation body type.

In this study, numerical simulations are employed to optimize the method since there are only few works that used this approach to address the problem. Therefore, through numerical simulation, the optimization results are more effective by reducing the time and number of prototypes to be constructed. Hence, numerical are one of the essential tools for this type of investigation. Ansys® Workbench as a commercial numerical simulation was utilised to solve the problem by using the Finite Element Method (FEM). For this purpose, the Application Customization Toolkit (ACT) of PiezoAndMEMS® (V18.0) was added. Table 2 summarizes the material properties used in this study.

The above material parameters are used for the model analysis in ANSYS. As can be seen, the piezoelectric coefficient, e31, and dielectric constant, e33, represent the effectiveness of converting mechanical to electrical energy via the coupling mode, as mentioned in Eqs. (3) and (4).

3. Results and discussions

3.1. Numerical results

The first simulation tests were performed to determine the resonance frequency of the flexible piezoelectric cantilever beam for three proposed models. Since the resonant vibrations amplify the relative displacement due to piezoelectric material being compressed, electrical power can be generated. Fig. 5 depicts the numerical simulation process including result of deformation distribution for three models; rectangular, trapezoidal, and stingray, considering the mass free at the end of the cantilever.

Since the objective of this study is to design a multiple blade model, the single blade of proposed FHP was not included in this simulation. To understand the effectiveness of the simulation, the variation of deformation is produced by simulating all 5 blades from different models. In addition, three attempt factors are obtained from numerical methods, which are thickness (T), length (L), and number of blades (n), to determine the suitable impact factor in Section 3.2. Furthermore, these factors are being used in statistical analysis to further investigate which are suitable designs. Fig. 6 (a-e) illustrates result deformation graphs along models created by varying the length and fixing the thickness on FHP for all the considered models with the following geometric parameters: n blades, $T = 0.2$ *mm*, $L = 60 - 300$ *mm*.

As can be seen, a smooth decrease in the f_r with an increase in the length. This finding indicates that larger flexible blade lengths require smaller deformations of f_r. Therefore, an increment in the blade length will lead to a decrease in the resonance. Furthermore, the curve depicts the effect of single parameters; length, are remains sensible when multiple n increased. The result indicates that the structure's response also has an influence on the length of FHP and this agrees with similar findings reported by other researchers [21,28].

Regarding the curves displayed in Fig. 6, it is possible to conclude that a stingray has a lower value of deformations; nonetheless, by increasing the area accessible for energy extraction, the deformations are spread practically equally throughout the cantilever beam surface. However, this can be proved through the Analysis of Variance (ANOVA). To understand the effectiveness of another design factor, deformations of variance thickness was validate using numerical ANSYS. Fig. 7 (a-e) shows the deformation graphs using the models created by varying the thickness and fixing the length on FHP for all of them, with the following geometric parameters: $T = 0.2 - 1{,}0$ *mm*, $L = 300$ *mm* and n blades.

Generally, thickness increased with f_r as well as deformation. It can also been seen that the thickness of the stingray increases slowly at the lower f_r compared with the rectangular and trapezoidal one due to having a smaller average of deformation. In addition, the areas available for energy extraction are larger since deformation is distributed along the entire beam surface. Overall, the obtained result for the influence of thickness content on deformation supports the proposed model.

Hence, the input factor and numerical result are shown in Table 3. As mentioned in Fig. 6, lower f_r are associated with the length; 300 mm for all model. Selection lengths is fixed at 300 mm and were chosen with orthogonal array, L_{27} test results; 9 readings for each shape by run in ANSYS were tested in ANOVA to select the best design.

It gives support that the following approximation can be used to determine the resonance of deformation at various factors.

3.2. Optimization strategy

Apart from this, the predefined conditions of the energy harvester are required to optimise the output responses. Hence, the goal of this research is to combine simulation-based analysis with optimization methods to get the desired output. In addition, design of experiment (DOE) methods is performed using statistical analysis to gain the

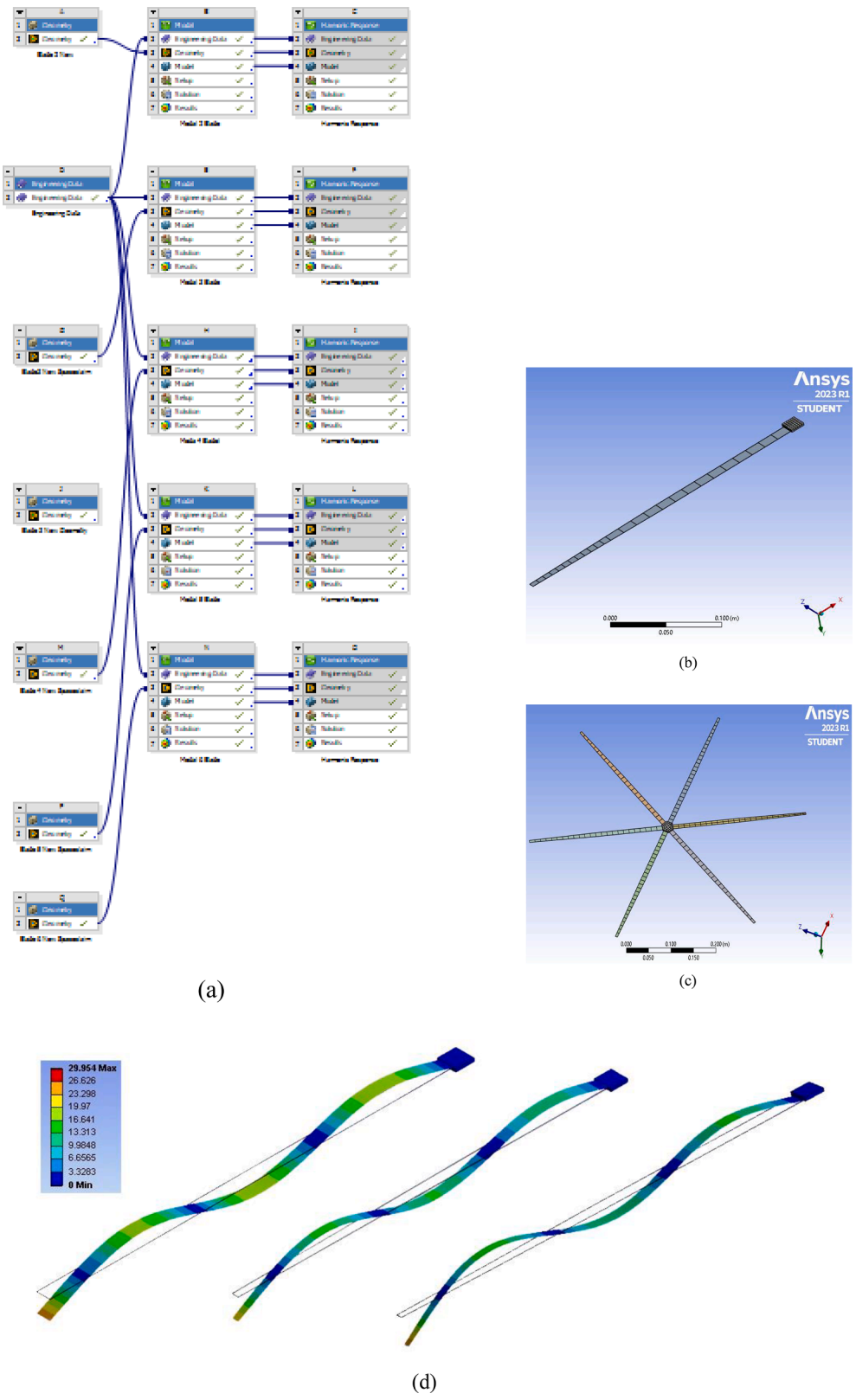

Fig. 5. Numerical simulation on ANSYS; (a) Workbench platform to create and simulate design model, (b) Meshing process for single blade, (c) Meshing process for multiple blade and, (d) Deformation distributions on the beam surface for FHP model.

optimised value of the controllable factors. Therefore, to optimize the design parameters for flexible blades, Minitab® software with version 18.1 is used, using a statistical analysis method based on Taguchi and ANOVA.

Table 4 depicts a summary of the control factors which were carried out with the three levels of controllable factors; T_1, T_2, and T_3 to define as variable during analysis. The maximum number of blades used is 6 to define the maximum availability of output energy. The maximum L is

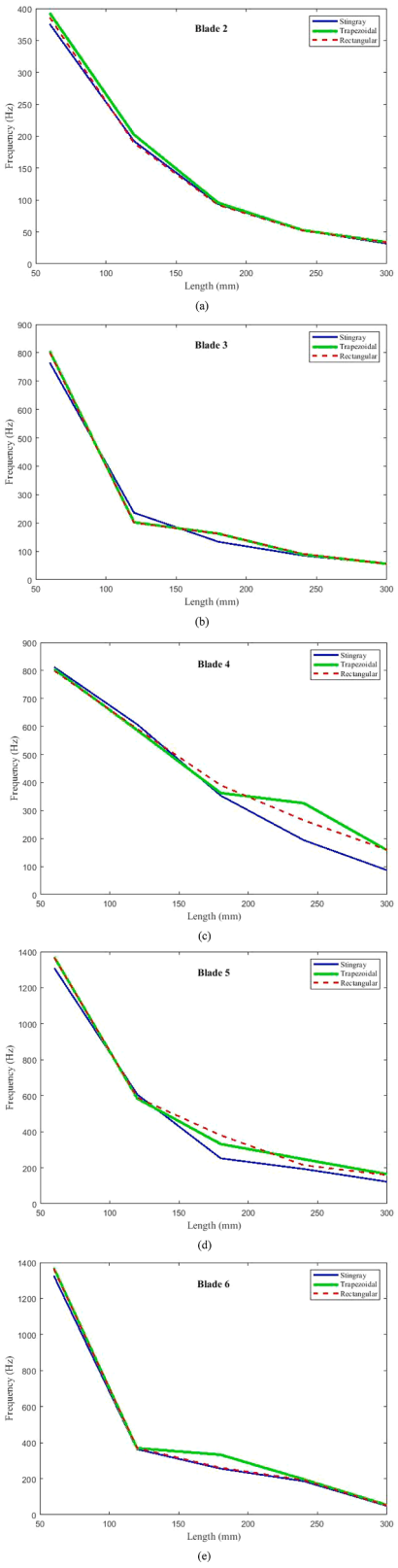

Fig. 6. Deformation of FHP model; trapezoidal, rectangular and stingray along L varied from 60 – 300 mm and $T = 0.2$ mm.

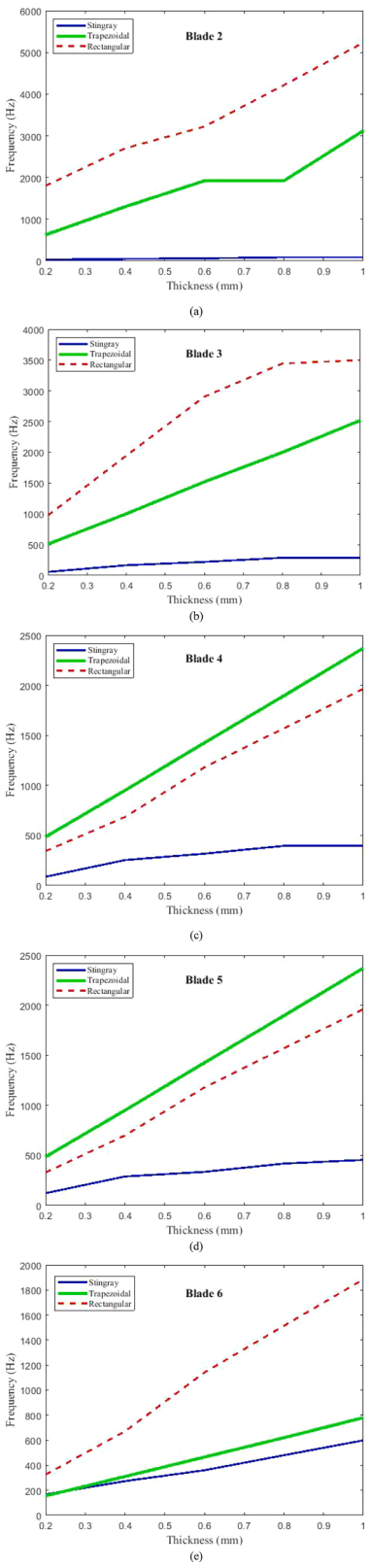

Fig. 7. Deformation of FHP model; trapezoidal, rectangular and stingray along T varied from 0.2 – 1.0 mm and $L = 300$ mm.

300 mm and T is 1.0 mm.

The procedure of determining quality factors is divided into two parts. The first part is to discover the design characteristics that decrease variability and their values. The second part requires us to choose the factor that will attempt to get the mean values closer to the objective point.

Table 3
Numerical result for L = 300 mm; L_{27} orthogonal array with rectangular (shape 1), trapezoidal (shape 2) and stingray blade (shape 3).

Shape	No. of Blade	Thickness (mm)	Frequency (Hz)
1	2	0.2	1800
1	2	0.6	3221
1	2	1.0	5232
1	4	0.2	343
1	4	0.6	1180
1	4	1.0	1965
1	6	0.2	325
1	6	0.6	1141
1	6	1.0	1885
2	2	0.2	625
2	2	0.6	1920
2	2	1.0	3120
2	4	0.2	485
2	4	0.6	1425
2	4	1.0	2370
2	6	0.2	155
2	6	0.6	465
2	6	1.0	780
3	2	0.2	32
3	2	0.6	62
3	2	1.0	87
3	4	0.2	87
3	4	0.6	318
3	4	1.0	396
3	6	0.2	167
3	6	0.6	360
3	6	1.0	599

Table 4
Control factor; L_1, L_2, and L_3 with their levels.

Control factor	T_1	T_2	T_3	Type
Blade	2	4	6	-
Length (mm)	60	180	300	-
Thickness (mm)	0.2	0.6	1	-
Shape	-	-	-	1
	-	-	-	2
	-	-	-	3

3.3. Taguchi's DOE

Taguchi is a statistical method that aims to improve the quality of design performance. This includes the output system's response to changes in various parameters that are correlated in some way. It is based on statistical analysis, which investigates how responsive the goal variables are to the input factors in an effort to enhance the effectiveness of the output or design. The Taguchi approach is best suited for systems whose ideal operating conditions rely on many input parameters that are connected with one another. Each parameter's impact on the Taguchi method system is comparable to the signal-to-noise ratio [26].

Furthermore, Taguchi approach has been widely used to check the influence of individual factors and minimise the manufacturing lead time on energy harvesting [27]. Taguchi's DOE reduces the influence of noise factors and use them as a controllable factor in the response of a system. In addition, it explains how the responsiveness of a system differs comparatively under various design choices. Taguchi's analyses estimated the influence of controllable factors through S/N ratio and response chart by quality factors. The process of quality factors is completed in two steps; first, identify the design parameters with their levels that reduce variability; second, need to select factors that carry means value close to the goal point.

Therefore, three categories of goal in S/N; *smaller is better, nominal is better*, and *larger is better*. Because the purpose of this research is to achieve the minimum value of f_r as deformation, the *smaller is better* feature is applied in this study. The selection of $L = 300$ mm as the first identified design parameter since the result deformation from Fig. 6 shows that the minimum frequency is recorded for each model. Besides, this also analyses the suitable blade design by using Taguchi to gauge the impact of controllable boundaries on energy harvesting. L_{27} orthogonal array with three controllable factors, such as those shown in Table 3 and Table 4, is used to acquire the best value of the parameter in order to attain maximum energy harvester.

Fig. 8 shows how the output response of the control factor from Taguchi analysis can be varied along the S/N ratio and means plots. As can be seen in Fig. 8 (a), deformation decreases for the stingray model compared with the rectangular and trapezoidal. This is because design tappered attracted the minimum f_r of FHP respectively agreed with the findings of the literature [29]. In addition, a higher number of blades will lead to an increase of deformation. This is owing to the increasing number of the individual blades for each design. Furthermore, it was observed that deformation increases as the thickness increases. This is due to the effect of length on self-deformation of the f_r studied.

Considering the fact that reducing the thickness will affect the actual resonance of the cantilever beam. The results are in agreement with similar findings reported by other researchers [21]. The obtained S/N ratio response table for the FHP is shown in Table 5. Fig. 8 (b) shows the mean S/N ratio graph obtained using Minitab software. A higher S/N ratio represents a difference minimum variation of measured output and desirable output. Besides, the highest mean S/N ratio obtained for FHP are S is 3; stingray model, number of blade at 6 and thickness at 0.2 mm respectively. Furthermore, the predicted optimum process parameters for obtaining the deformation of f_r using the Taguchi method are found as $S = 3$; stingray, $n = 6$; number of blades, and $T = 0.2$ mm. Table 5 depicts the corresponding level values for easy understanding from the response table.

3.4. ANOVA's approach

ANOVA is a numerical method for utilising the factor of individual influence in independent variables on piezoelectric energy harvesting output. The ANOVA method was used in this study to verify the results of the Taguchi analysis. These optimization step and approaches are highlighted in Fig. 9.

Since the approaches in Taguchi proposed that stingray model has predicted to be optimum for harvesting energy, ANOVA are utilized to verify the results of the Taguchi analysis. Besides, ANOVA identifies the process variable that affects the most performance parameters. The present analysis is conducted by defining the interval estimation and significant of 95 % confidence level and 5 % of risk level; α (for a 95 % confidence interval α equal to 0.05, hence 5 %). The purpose of this analysis is to determine the p-value for each factor and variable. The factor and variable with the lowest p-value will be more effective in producing the best output response. Table 6 presents the ANOVA result of stingray model for the S/N ratio with a 95 % confidence level.

After the investigation, it is observed that the factor with *P-Value* less than risk level of 0.05 is a significant factor; shape, thickness and blade of the stingray model. Besides, Table 7 depicts a summary of the comparative model for stingray. In the view of the results obtained, the design modeling can achieve 90.74 % of R-sq. which means the design factor that was affected in Table 6 is accepted.

Therefore, the record of R-sq; 90.74 % is an acceptable design as it is close to one. In addition, if close to one, it reveals that each variable is satisfied between the dependent and independent variables.

The regression analysis propagates the linear connection between the independent and dependent variables of the stingray blade. The prediction equation was obtained through regression analysis as shown in Eq. (13) respectively for stingray model.

$$f_{FHP} = 148 - 2.27\ L + 1046\ T + 75.2\ n\ R^2 = 90.74\ \% \tag{13}$$

where L is length, T is thickness and n number of blades.

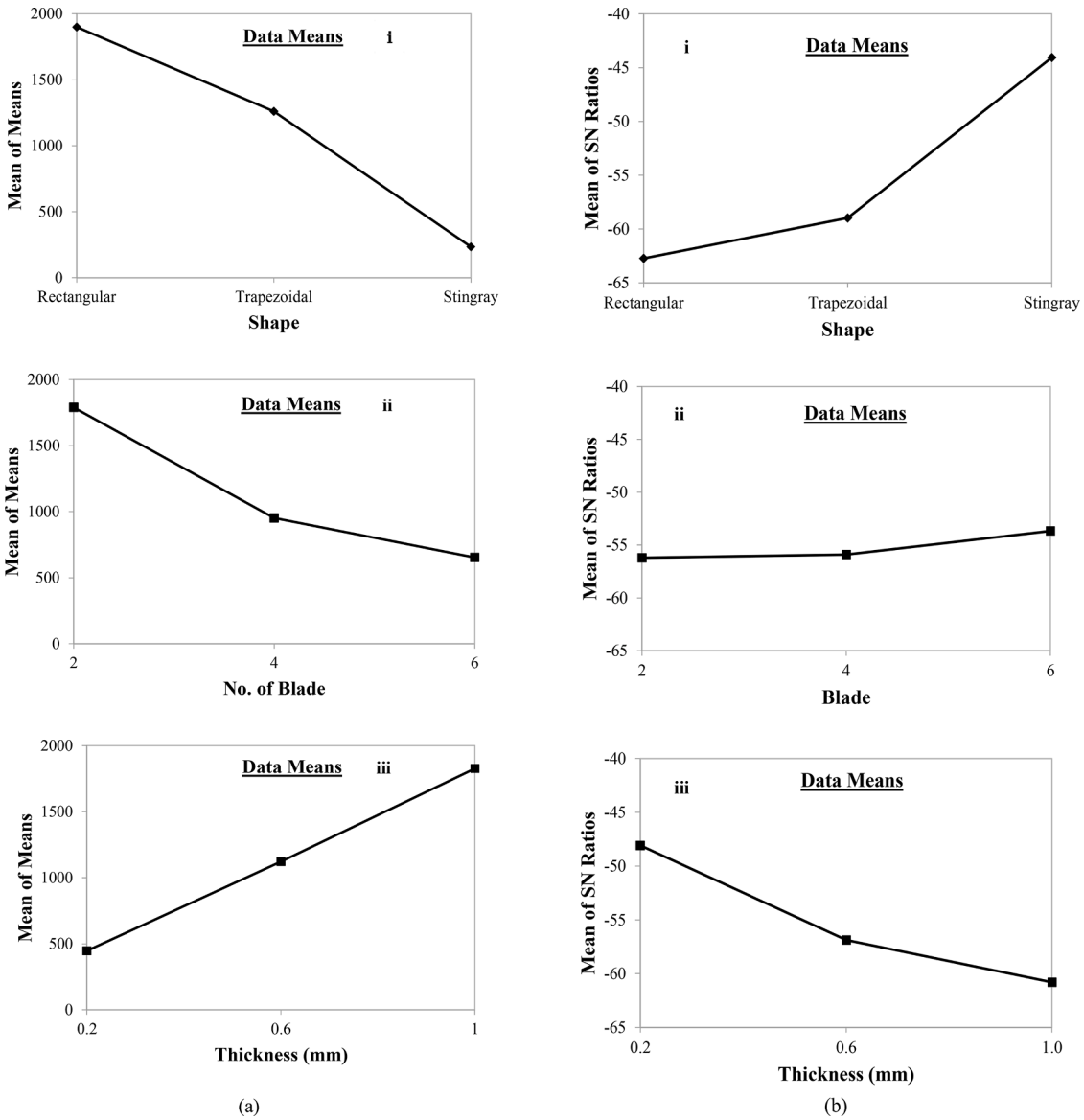

Fig. 8. Effect of FHP energy harvesting; (a) means values (b) S/N ratio.

Table 5
Response table via S/N ratio and mean values.

		Means S/N Ratio			
Symbol	Process Parameters	L1	L2	L3	Rank
S	Shape	-62.73	-58.97	**-44.07**	1
T	Thickness	**-48.08**	-56.88	-60.80	2
n	Blade	-56.2	-55.9	**-53.67**	3

Linear relationship between dependant variable and independent variable of FHP are interpolated by regression analysis. Furthermore, it depicts how the value of response variable changes with the independent variable. Confirmation test were conducted using Eq. (13) to validate the three factor of independent variable; *L, T* and *n* respectively.

Fig. 10 shows the regression analysis variation in output voltage with different independent variables. As can be seen, the length and number of blades are proportional to the output voltage, while the thickness decreases with higher voltage. In addition, it is anticipated that voltage will be higher by increasing the factor of blade and length. R^2 constantly exceeds 85% for better regression with a voltage recorded of 184.78 mV and 1230.6 mV for length and blade deformations as shown in Fig. 10 (a) and (b). In Fig. 10 (c), the voltages decrease with increased thicknesses, with a maximum of 185 mV recorded. This finding is owing to a deformation of f_r resulting in a significant factor of harvester, which in turn generates electrical output on the FHP. From the confirmation result, it was found the result followed within the given range parameters. In the literature, the trend was also in agreement with similar finding reported by other researches [21,28].

Fig. 11 shows the individual relationship between voltage and f_r for the stingray model. In general, the self-resonance frequency was recorded at 160.32 Hz. The peak voltage at single resonance was 184.78 mV, with an average power of 17.07 $\mu W/mm^2$. Thus, the output energy is optimised once the deformations of the FHP generator are maximized. In conjunction with the design, as the frequency recorded will be affected by the input factor, the excitation frequency exceeds the resonance frequency.

Table 8 presents the comparison strategy and method application in this work in relation to the other works already mentioned. From there, it is possible to state that the method optimization for this research is possible to affirm that the power generated in this work is acceptable. Furthermore, the novelty of this research has been validated as useful in

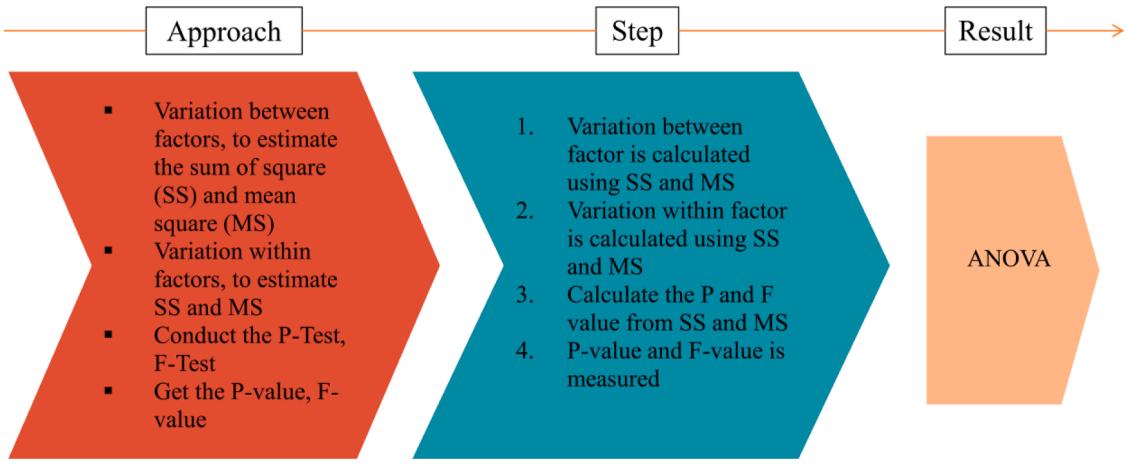

Fig. 9. Optimization step and approach for ANOVA method.

Table 6
ANOVA table for FHP with *P-Value* less than risk level; α = 0.05.

Source	DF	Add SS	Adj MS	F-Value	P-Value	Significant
Shape	2	1.27E+07	6.35E+06	10.08	0.001	Significant
Blade	2	6.20E+06	3.12E+06	4.95	0.018	Significant
Thickness	2	8.56E+06	4.28E+06	6.8	0.006	Significant
Error	20	1.26E+07	6.30E+05	-	-	-
Total	26	4.01E+07	-	-	-	-

Table 7
Summary of FHP energy harvester with R-sq; 90.74 % for stingray model.

S	R-sq	R-sq(adj)	R-sq(pred)
58.3136	90.74%	86.11%	77.40%

comparison to previous studies.

As beneficiaries, the propose energy harvester is expected to replace conventional methods of supplying the energy demand of normal operations in home appliances and one of the initiative to support green-environmental promising technology. Furthermore, because the device is simple to install, construct, and maintain, there are no special constraints if it is used in real-world applications.

4. Conclusions

In this work, piezoelectric ceramics (PZT) was studied, and experiments were designed using the Taguchi and ANOVA methods in order to assess the effect of length, thickness, and shape on the mechanical properties. From the effect of resonance frequency on design properties, the numerical method suggested that the optimum conditions can be obtained by using six blades on the stingray model. Besides, in this investigation, it was shown that the harvesters were still able to generate output power by using the piezoelectric effect d_{31}, even with low results, which were easily employed through design. Therefore, future work should focus on the development of prototypes and products for practical application. Other methods to increase material size include large-scale production to satisfy the demand and increase output energy.

Declaration of Competing Interest

The authors declare that they have no known competing financial interests or personal relationships that could have appeared to influence the work reported in this paper.

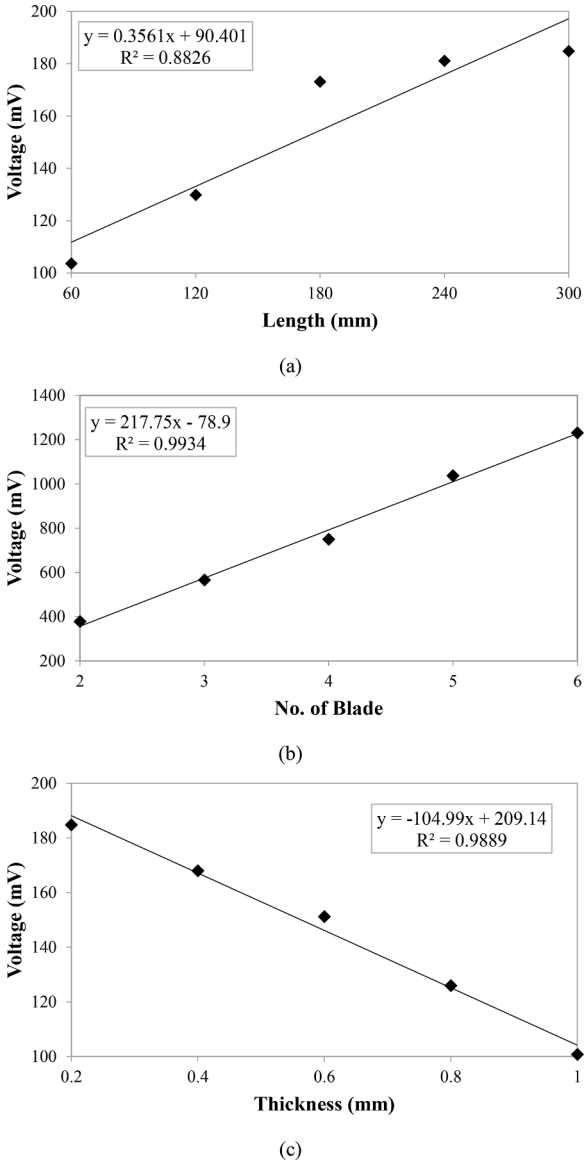

Fig. 10. Regression analysis for output voltage with (a) length; $R^2 = 0.8826$ (b) blade; $R^2 = 0.9934$ and (c) thickness; $R^2 = 0.9889$.

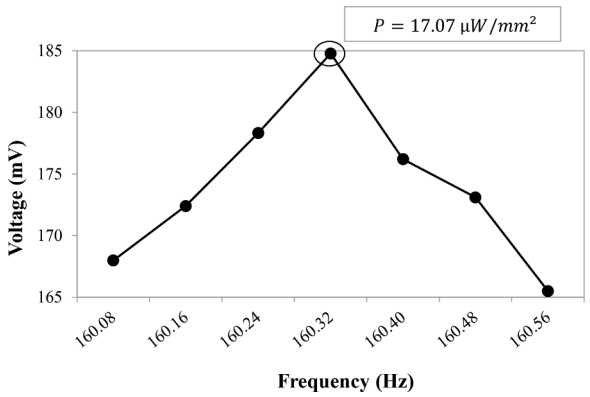

Fig. 11. Relationship between voltage and f_r with maximum power 17.07 μW/mm^2 at 160.32 Hz.

Table 8
Comparison between strategy and method application in this work with other devices present in the literature.

Applications	Strategy Developed	Method Optimization	Refs.
Mass-spring floating energy harvester	Use piezoelectric effect to harvest energy from intermediate and deep water	Developed mathematical model bade on Lagrangian-Euler method and solve using iteration method to calculate RMS of electric power	[23]
Magnet tip-mass with tube metal ball positioning for sway movement	Multi-directional vibration with low frequency by applying in buoys and boats	Experimental devices with different parameters optimization	[2]
Two horizontal cantilever plate and fixed on vertical rectangular column	Use piezoelectric effect to harvest energy from transverse wave motion	Developed mathematical model according to airy linear wave theory and elastic beam model to calculate RMS of electric power	[19]
Cantilever substrate with proof mass on ocean bed	Use piezoelectric effect of piezoelectric patch to harvest energy from longitudinal wave motion	Developed mathematical model through airy linear wave theory and classical elastic beam model to calculate RMS of electric power	[22]
Painted and laminate flexible piezoelectric for wave energy	Tip deformation rate of flexible device for intermediate wave to harvest energy	Experimental devices with different parameters optimization	[24]
Flexible piezoelectric on surface of sea wave	Use piezoelectric effect for multiple blade to harvest energy on surface of sea wave	Developed numerical simulation using ANSYS to propose model and verify through Taguchi and ANOVA to approach design of experiment	Propose research

Data availability

The authors are unable or have chosen not to specify which data has been used.

Acknowledgement

This research is funded by the Universiti Malaysia Pahang (UMP) through Postgraduate Research Grant Scheme (PGRS) PGRS200319.

References

[1] A. Rahman, O. Farrok, M. Haque, Environmental impact of renewable energy source based electrical power plants : Solar, wind, hydroelectric, biomass, geothermal, tidal, ocean, and osmotic, Renew. Sustain. Energy Rev. 161 (2022), 112279, https://doi.org/10.1016/j.rser.2022.112279.
[2] W.S. Hwang, J.H. Ahn, S.Y. Jeong, H.J. Jung, S.K. Hong, J.Y. Choi, J.Y. Cho, J. H. Kim, T.H. Sung, Design of piezoelectric ocean-wave energy harvester using sway movement, Sensors Actuators A Phys. 260 (2017) 191–197, https://doi.org/10.1016/j.sna.2017.04.026.
[3] S. Zhou, M. Lallart, A. Erturk, Multistable vibration energy harvesters: principle, progress, and perspectives, J. Sound Vib. 528 (2022), https://doi.org/10.1016/j.jsv.2022.116886.
[4] A. Afsharfard, H. Shin, S. Hosseini, E.S. Kim, I. Lee, K.C. Kim, Design of vibro-impact electromagnetic ocean-wave energy harvesting system; an experimental study, Ocean Eng. 263 (2022), 112168, https://doi.org/10.1016/j.oceaneng.2022.112168.
[5] M. Melikoglu, Current status and future of ocean energy sources: a global review, Ocean Eng. 148 (2018) 563–573, https://doi.org/10.1016/j.oceaneng.2017.11.045.
[6] Z. Lin, Y. Zhang, Dynamics of a mechanical frequency up-converted device for wave energy harvesting, J. Sound Vib. 367 (2016) 170–184, https://doi.org/10.1016/j.jsv.2015.12.048.
[7] H. Pan, L. Qi, Z. Zhang, J. Yan, Kinetic energy harvesting technologies for applications in land transportation: a comprehensive review, Appl. Energy 286 (2021), 116518, https://doi.org/10.1016/j.apenergy.2021.116518.
[8] P. Wave, Pelamis : experience from concept to connection, (2012), 365–380, 10.1098/rsta.2011.0312.
[9] F. Qian, Y. Liao, L. Zuo, P. Jones, System-level finite element analysis of piezoelectric energy harvesters with rectified interface circuits and experimental validation, Mech. Syst. Signal Process. 151 (2021), 107440, https://doi.org/10.1016/j.ymssp.2020.107440.
[10] Z.H. Lai, G. Thomson, D. Yurchenko, D.V Val, E. Rodgers, On energy harvesting from a vibro-impact oscillator with dielectric membranes, Mech. Syst. Signal Process. 107 (2018) 105–121, https://doi.org/10.1016/j.ymssp.2018.01.025.
[11] M. Bedier, D. Galayko, A 100nW power overhead load interface for electrostatic vibrational energy harvester with a high biasing voltage, Procedia Eng. 168 (2016) 1693–1697, https://doi.org/10.1016/j.proeng.2016.11.492.
[12] N. Sezer, M. Koç, Nano energy a comprehensive review on the state-of-the-art of piezoelectric energy harvesting, Nano Energy 80 (2021), 105567, https://doi.org/10.1016/j.nanoen.2020.105567.
[13] G. Shi, D. Tong, Y. Xia, S. Jia, J. Chang, Q. Li, X. Wang, H. Xia, Y. Ye, A piezoelectric vibration energy harvester for multi-directional and ultra-low frequency waves with magnetic coupling driven by rotating balls, Appl. Energy 310 (2022), 118511, https://doi.org/10.1016/j.apenergy.2021.118511.
[14] N. Wu, Q. Wang, X.D. Xie, Ocean wave energy harvesting with a piezoelectric coupled buoy structure, Appl. Ocean Res. 50 (2015) 110–118, https://doi.org/10.1016/j.apor.2015.01.004.
[15] S. Kazemi, M. Nili-Ahmadabadi, M.R. Tavakoli, R. Tikani, Energy harvesting from longitudinal and transverse motions of sea waves particles using a new waterproof piezoelectric waves energy harvester, Renew. Energy 179 (2021) 528–536, https://doi.org/10.1016/J.RENENE.2021.07.042.
[16] H.S. Kim, J.H. Kim, J. Kim, A review of piezoelectric energy harvesting based on vibration, Int. J. Precis. Eng. Manuf. 12 (2011) 1129–1141, https://doi.org/10.1007/s12541-011-0151-3.
[17] A. Jbaily, R.W. Yeung, Piezoelectric devices for ocean energy: a brief survey, J. Ocean Eng. Mar. Energy 1 (2015) 101–118, https://doi.org/10.1007/s40722-014-0008-9.
[18] R. Ahmed, F. Mir, S. Banerjee, A review on energy harvesting approaches for renewable energies from ambient vibrations and acoustic waves using piezoelectricity, Smart Mater. Struct. 26 (2017), 085031, https://doi.org/10.1088/1361-665X/aa7bfb.
[19] X.D. Xie, Q. Wang, N. Wu, Potential of a piezoelectric energy harvester from sea waves, J. Sound Vib. 333 (2014) 1421–1429, https://doi.org/10.1016/j.jsv.2013.11.008.
[20] Y. Cui, H. Wang, M. Li, K. Sun, Simulation of wave energy harvesting by piezoelectric seaweed, IOP Conf. Ser. Mater. Sci. Eng. 250 (2017), https://doi.org/10.1088/1757-899X/250/1/012022.
[21] Q. Zhao, Y. Liu, L. Wang, H. Yang, D. Cao, Design method for piezoelectric cantilever beam structure under low frequency condition, Int. J. Pavement Res. Technol. 11 (2018) 153–159, https://doi.org/10.1016/j.ijprt.2017.08.001.
[22] X.D. Xie, Q. Wang, N. Wu, Energy harvesting from transverse ocean waves by a piezoelectric plate, Int. J. Eng. Sci. 81 (2014) 41–48, https://doi.org/10.1016/j.ijengsci.2014.04.003.
[23] N.V Viet, X.D. Xie, K.M. Liew, N. Banthia, Q. Wang, Energy harvesting from ocean waves by a floating energy harvester, Energy 112 (2016) 1219–1226, https://doi.org/10.1016/j.energy.2016.07.019.
[24] H. Mutsuda, Y. Tanaka, Y. Doi, Y. Moriyama, Application of a flexible device coating with piezoelectric paint for harvesting wave energy, Ocean Eng. 172 (2019) 170–182, https://doi.org/10.1016/j.oceaneng.2018.11.014.
[25] J. Hennig, M. Peric, Computation of flow-induced motion of floating bodies, Appl. Math. Model. 29 (2005) 1196–1210, https://doi.org/10.1016/j.apm.2005.02.014.
[26] E. Al, X. Wang, R. Zhang, L. Zuo, A parameter study and optimization of two body wave energy converters, Renew. Energy 131 (2019) 1–13, https://doi.org/10.1016/j.renene.2018.06.117.

[27] M.A. Sheeraz, Z. Butt, A.M. Khan, S. Mehmood, A. Ali, M. Azeem, A. Nasir, T. Imtiaz, Design and optimization of piezoelectric transducer (PZT-5H Stack), J. Electron. Mater. 48 (2019) 6487–6502, https://doi.org/10.1007/s11664-019-07453-7.
[28] A.G. Paulo e Silva, J.M. Basílio Sobrinho, C. da Rocha Souto, A. Ries, A.C. de Castro, Design, modelling and experimental analysis of a piezoelectric wind energy generator for low-power applications, Sensors Actuators A Phys 317 (2021), https://doi.org/10.1016/j.sna.2020.112462.
[29] H. Li, C. Tian, Z.D. Deng, Energy harvesting from low frequency applications using piezoelectric materials, Appl. Phys. Rev. 1 (2014) 0–20, https://doi.org/10.1063/1.4900845.

Ahmad Syafiq Deraman is currently doing his Ph.D at Universiti Malaysia Pahang (UMP). Previously, he was a lecturer at DRB-HICOM University of Automotive Malaysia. He has vast experience as automotive engineers as he spent more than 6 years in in Automotive Manufacturing at Proton Tanjung Malim Sdn Bhd. Mr Deraman holds B,Eng of Electrical Engineering from UMP and Master in Mechatronic Engineering from Universiti Malaya.

Mohd Rusllim Mohamed was awarded his Ph.D. from Universiti Malaysia Pahang (UMP) in 2013. Previously, he completed M.Eng. Electrical Eng. from Universiti Teknologi Tun Hussein Onn (UTHM), Malaysia in 2004, B.Eng. Electronic Eng. from the University of Warwick, UK in 2001, and a Diploma in Electrical Eng. (Power Systems) from Universiti Teknologi Mara (UiTM), Malaysia in 1998 respectively. He used to be a fellow researcher at the University of Duisburg-Essen, Germany in 2004 and the University of Southampton, UK from 2008-2010. As an academician, he is now a Professor at the Universiti Malaysia Pahang (UMP) and an active member of the Sustainable Energy & Power Electronics Research (SuPER) Cluster, which he leads one of the sub-cluster i.e. The Sustainable Energy Group (SEG). Dr. Rusllim involves in technical research for energy harvesting and energy storage-specifically redox flow battery (RFB). His other research interests include electric vehicles, renewable energy, soft computing, engineering education, and Technical and Vocational Education and Training (TVET). In 2019, he has been appointed as visiting Professor at Yildiz Technical University, Turkey.

Wan Ismail Ibrahim received his PhD (Electrical) from Universiti Malaysia Pahang (UMP) in 2021. Previously, he completed M.Eng Electrical (Power) and B. Eng. Electrical (Electronics) from Universiti Teknologi Malaysia (UTM) and Universiti Malaysia Pahang (UMP) in 2010 and 2007 respectively. He is currently a senior lecturer at Faculty of Electrical & Electronics Engineering Technology Universiti Malaysia Pahang (UMP). He is the author and co-author of more than 25 publication in international journals and proceedings. His research interests include all area in renewable energy, power electronics converter, lightning localised system and electrical power system optimisation.

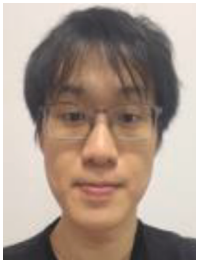

Puiki Leung is a Professor in the School of Energy and Power Engineering at the University of Chonqing, China. He holds a BEng in Engineering Sciences (Mechanical Engineering) and a PhD in Electrochemical Engineering from the University of Southampton. His PhD project focused on the development of a zinc-cerium redox flow batteries. After my graduation, he has held a number of research positions in several universities/institutions (e.g., Oxford, Warwick, Southampton, Hong Kong) in the areas of energy storage and material processing. His research interests lie in the fields of electrochemical devices, mathematical modelling, mechanical testing and novel characterization/manufacturing techniques. He has been also awarded 3 prestigious fellowships (~ £ 800 k) in Europe and China.